SSRG International Journal of Electronics and Communication Engineering
ISSN: 2348-8549/ https://doi.org/10.14445/23488549/IJECE-V13I1P108

Volume 13 Issue 1, 89-98, January 2026

Original Article

Design and Analysis of a Spectrally Efficient Adaptive Polarization-Multiplexed OFDM System Using Novel CSD Code Encoding

Chetan R Chauhan[1], Pravin R Prajapati[2]

[1]*Gujarat Technological University, Gujarat, India.*
[1]*SPB Patel Engineering College, Gujarat Technological University, Gujarat, India.*
[2]*A D Patel Institute of Technology, The Charutar Vidya Mandal (CVM) University, New Vallabh Vidhyanagar, Gujarat, India.*

[1]*Corresponding Author : chetan.svit@gmail.com*

Received: 05 November 2025 Revised: 07 December 2025 Accepted: 06 January 2026 Published: 14 January 2026

Abstract *- This paper introduces a spectrally efficient adaptive polarization-multiplexed OFDM system that uses a short, low-cross-correlation CSD code. It also incorporates hybrid optical amplifiers to improve multi-user performance. The proposed CSD code offers a short code length with negligible cross-correlation. The adaptive polarization-multiplexing method then adjusts the polarization phase difference and the power split ratio based on receiver feedback. Together, these techniques increase user capacity and reduce BER. This adaptive process also lowers polarization-dependent loss and balances power between polarization states. As a result, it improves SNR and achieves a lower Bit Error Rate compared to conventional polarization-multiplexing schemes. The simulations demonstrate the practical feasibility of the proposed system by successfully recovering user data. The analytical results further show that, at a per-user rate of 622 Mbps, the system can accommodate up to 184 users at a BER of 10^{-9}. This represents a 72% and 84% increase in capacity compared to existing ZCC, MDW, and FCC-coded OFDM-OCDMA systems. These gains are achieved using advanced adaptive polarization multiplexing combined with CSD coding. Optimal system performance occurs at a balanced polarization split ratio, $\alpha = 0.5$, and zero phase difference, $\phi = 0°$, with deviations significantly reducing capacity. By combining CSD coding, adaptive polarization control, and hybrid amplification, the system achieves higher spectral efficiency and improved scalability. It also delivers robust performance under diverse operating conditions. Collectively, these features highlight its potential as an effective solution for next-generation, high-bandwidth optical access systems. The system can adapt in real time to changing channel conditions, varying network loads, and operational disturbances.*

Keywords *- Adaptive polarization multiplexing, BER Optimization, CSD Code, Hybrid Amplifiers, OFDM- Spectral Encoding, PDL Mitigation.*

1. Introduction

The growing demand for high data rates and dense user support in 5G, IoT, and smart city networks. It has pushed optical communication systems to their limits [1]. Modern metropolitan infrastructures require high-bandwidth, ultra-reliable, and secure transmission to support applications such as autonomous vehicles, code key-based services, financial and defence hubs, and smart grids [1, 2]. These services share the same optical backbone, so the network must remain efficient and resistant to interference.

As user numbers increase, many existing coding and modulation methods begin to struggle. Their performance drops unless system complexity is increased. This challenge has encouraged the use of hybrid optical techniques that offer stable, scalable, and high-capacity operation in metropolitan networks.

2. Literature Review

Orthogonal Frequency Division Multiplexing – Spectral Amplitude Coding – Optical Code Division Multiple Access (OFDM-SAC-OCDMA) improves spectral efficiency through orthogonal subcarriers and unique code signatures. But it struggles with Multiple-Access Interference (MAI) in high-density scenarios [2, 3]. MAI becomes more severe when the number of active users exceeds the code cardinality, which increases the bit-error rate [3]. Zero Cross-Correlation (ZCC) codes [4] reduce MAI but require longer code lengths, leading to higher latency. Flexible Cross-Correlation (FCC) codes [5] use shorter lengths, but this results in higher cross-correlation. Both coding schemes are important for maintaining Quality of Service (QoS) in heterogeneous networks, especially when multiple service types share the same optical backbone [6]. The proposed novel Compact Spread Diagonal (CSD) codes

mitigate MAI with short lengths and negligible cross-correlation, enhancing reliability in hybrid fiber-optic systems [4, 5]. The CSD code enables higher user capacity and improved BER performance due to its code properties. Polarization multiplexing doubles system capacity by sending signals on orthogonal polarizations, but it introduces polarization-dependent loss and phase variations due to fiber impairments [7, 14]. In practical networks, temperature changes, mechanical stress, and wavelength-dependent birefringence make polarization stability harder to maintain [7, 8]. Adaptive Polarization Multiplexing (APM) dynamically adjusts polarization states to improve robustness in changing optical conditions. Hybrid Raman-EDFA amplifiers help reduce PDL through balanced gain, while controlling Amplifier Spontaneous Emission (ASE) noise remains important for long-haul transmission [9]. The system uses a broadband source that is highly sensitive to polarization effects. It is therefore limited to a short-distance metropolitan network. It is therefore limited to short-distance metropolitan networks. By using CSD codes, adaptive polarization-multiplexed OFDM-SAC encoding, and hybrid amplification, the system can support more users. This is done by improving spectral efficiency and lowering the required SNR in metropolitan area networks.

3. The System Architecture

The system begins with a broadband optical source that generates the wavelengths required for two users in an APM-based setup. At the transmitter, a polarization splitter separates the X-pol and Y-pol paths. Each path then optically modulates its respective user's OFDM electrical data using Mach–Zehnder Modulators (MZMs) as shown in Figure 1.

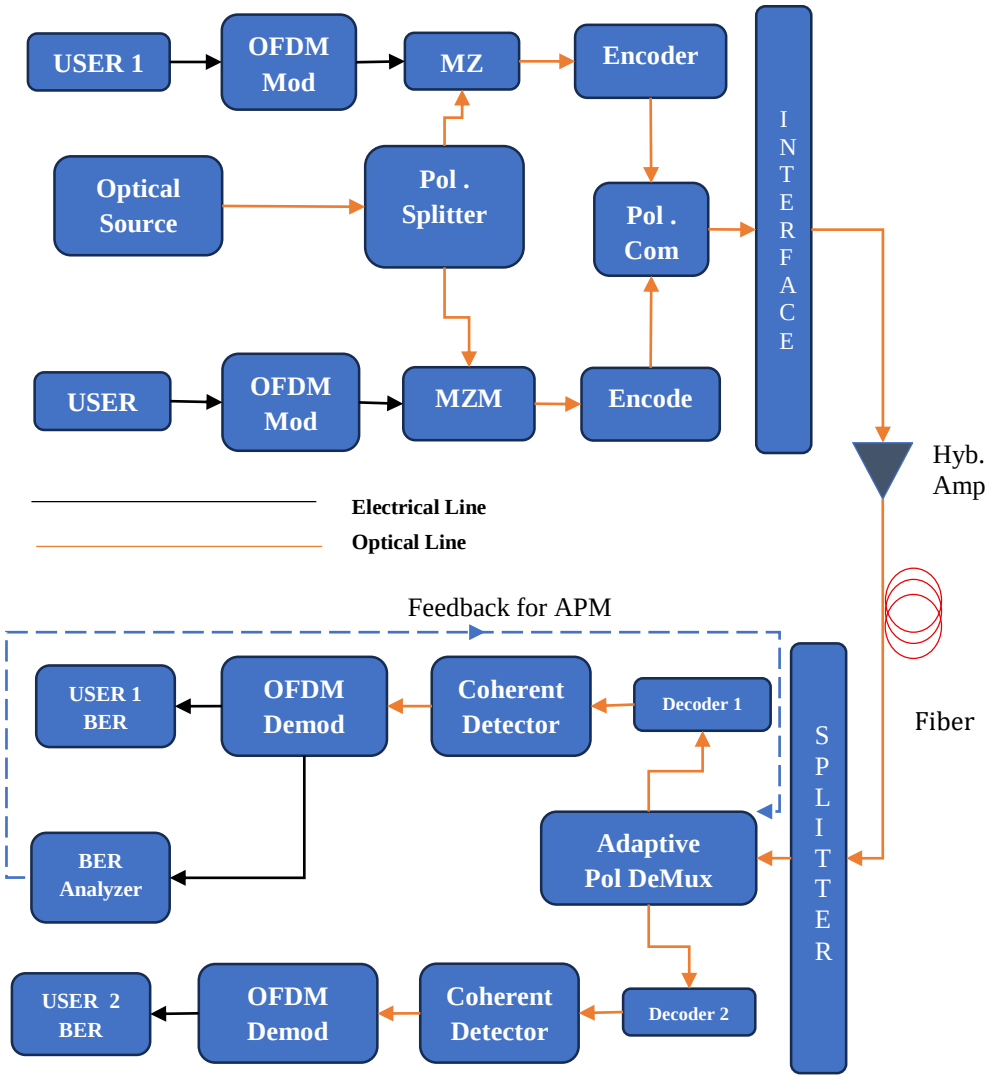

Fig. 1 System flow diagram

The SAC encoder spectrally shapes the modulated OFDM signal. The FBG chirp is kept broader than the electrical bandwidth. This ensures accurate spectral encoding and prevents distortion during the process. The modulated polarizations are recombined by a Polarization Beam Combiner. The combined signal is sent into the optical fiber link. The link uses hybrid EDFA and Raman amplification. The EDFA–Raman hybrid amplifier offers a wider operating wavelength range compared to other hybrid configurations, making it the most suitable choice for our system employing a broadband optical source [20].

Inline optical filters maintain SNR and PDL [9]. At the receiver, the optical signal is directed to an adaptive polarization-multiplexing block. The block adjusts the phase difference between the X-pol and Y-pol paths. It also adjusts the power split between the two polarizations. These changes are based on real-time feedback from the BER analyzer. This keeps the polarization states properly aligned.

The separated beams are decoded using FBGs to suppress Multiple-Access Interference (MAI), followed by coherent OFDM demodulation. The recovered electrical signals are monitored by a BER analyzer. An electrical constellation visualizer checks the signal quality and confirms clean QPSK constellations for accurate recovery.

3.1. The CSD Code Construction

The proposed CSD code architecture uses a structured decomposition into two orthogonal components. The data segment carries the user information channels, while the code-weight segment holds the signature sequences [5, 10].

The code construction is defined by the Weight (W) parameter used to optimize autocorrelation. It is also derived from the user Capacity (K), represented by a K×K diagonal matrix. This structure reduces cross-correlation while maintaining spectral efficiency. For K = 4,

$$\text{Diagonal Matrix} = \begin{bmatrix} 1 & 0 & 0 & 0 \\ 0 & 1 & 0 & 0 \\ 0 & 0 & 1 & 0 \\ 0 & 0 & 0 & 1 \end{bmatrix} \quad (1)$$

The proposed architecture constructs the data segment for K=4 and W=4 through a K×K matrix replicated |W/2|=2 times. The Code Segment (C) is synthesized using M diagonal submatrices of dimension (K/2) × (K/2) = 2 × 2 that undergo horizontal duplication |W/2| times. It is followed by vertical replication. The Data Segment [D] is represented as follows.

$$[D] = \underbrace{\begin{bmatrix} 1 & 0 & 0 & 0 & 1 & 0 & 0 & 0 \\ 0 & 1 & 0 & 0 & 0 & 1 & 0 & 0 \\ 0 & 0 & 1 & 0 & 0 & 0 & 1 & 0 \\ 0 & 0 & 0 & 1 & 0 & 0 & 0 & 1 \end{bmatrix}}_{\text{1 time}} \underbrace{\qquad}_{\text{2 time}} \quad (2)$$

$$\text{Code Segment} = [C] = \begin{bmatrix} 1 & 0 & 1 & 0 \\ 0 & 1 & 0 & 1 \\ 1 & 0 & 1 & 0 \\ 0 & 1 & 0 & 1 \end{bmatrix} \quad (3)$$

The ultimate CSD code Matrix (G) is represented

$$[G] = \begin{bmatrix} 1 & 0 & 0 & 0 & 1 & 0 & 0 & 0 & 1 & 0 & 1 & 0 \\ 0 & 1 & 0 & 0 & 0 & 1 & 0 & 0 & 0 & 1 & 0 & 1 \\ 0 & 0 & 1 & 0 & 0 & 0 & 1 & 0 & 1 & 0 & 1 & 0 \\ 0 & 0 & 0 & 1 & 0 & 0 & 0 & 1 & 0 & 1 & 0 & 1 \end{bmatrix} \quad (4)$$

The CSD code matrix allocates each row to base station users as unique code sequences. For example, Base Station 1 receives the sequence [1 0 0 0 1 0 0 0 1 0 1 0]. This corresponds to a code weight of four. The code length follows N = (K×W/2) + (K/2×W/2). The data transmission occurs on wavelengths λ1, λ5, λ9, and λ11 corresponding to logical '1's [13]. The code design ensures each sequence maintains exactly W/2 overlapping bits with only one other user, achieving negligible cross-correlation. This code structure enables efficient detection with low MAI. It achieves this by using a minimal code length and an optimized spectral cross-correlation distribution [3].

4. System Mathematical Model

To evaluate user capacity, the CSD OFDM-SAC-OCDMA system with adaptive polarization multiplexing is modeled using the BER parameter [15]. The SNR defines how reliable the transmission is. In OFDM systems, the SNR of each subcarrier strongly affects the overall BER. The BER depends on the number of users, the SNR, and the code cross-correlation [5, 6]. For an adaptive polarization-multiplexed OCDMA-OFDM system, the received SNR can be expressed as [5, 14]:

$$SNR = \frac{\langle I^2 \rangle}{\langle \sigma^2 \rangle} = \frac{\langle {I_p}^2 \rangle}{{\sigma_{sh}}^2 + {\sigma_{PIIN}}^2 + {\sigma_{th}}^2 + {\sigma_{ASE}}^2 + {\sigma_{IMD3}}^2} \quad (5)$$

To calculate the Signal-To-Noise Ratio (SNR) at the receiver, the following dominant noise sources are considered: (a) shot noise, (b) Phase-Induced Intensity Noise (PIIN), also referred to as Polarization-Dependent Loss (PDL), (c) thermal noise, (d) Amplifier Spontaneous Emission (ASE) noise, and (e) third-order intensity modulation. The novel CSD code's negligible cross-correlation effectively eliminates MAI noise from the system [15]. The spectral density of the received signal is expressed as in [5, 11].

$$I = \Re \int_0^\infty G(v) dv \cdot \sum_{n=1}^{K} C_n \cdot \exp^{j 2\Pi f_n t} \quad (6)$$

Here, $G(v)$ represents the Power Spectral Density (PSD) of a single pulse. The remaining term corresponds to the OFDM-modulated electrical signal for the n^{th} user transmitter

among a total of K subcarriers [6]. The receiver's total noise is indicated by

$$\sigma_{total}{}^2 = \sigma^2{}_{sh} + \sigma^2{}_{th} + \sigma^2{}_{ASE} + IMD_3$$

It is represented as,

$$\sigma_{total}{}^2 = \begin{pmatrix} 2eBI + \underline{I}^2 B\tau_c + 2n_{sp}hv(G-1)B + \\ IMD_3 + \frac{4K_b T_n B}{R_L} \end{pmatrix} \quad (7)$$

The parameters in Equation (3) can be interpreted as follows,
I denote the detector average photocurrent,
h refers to the plank's constant,
K_b represents the Boltzmann constant,
n_{sp} is the spontaneous emission factor,
T_n indicates the absolute temperature of the receiver,
B is the receiver's electrical bandwidth, and
R_L denotes the load resistance of the receiver.
During a single bit interval, PSD [5, 10] is

$$\int_0^\infty G(v)\,\mathrm{dv} = \int_0^\infty \left[\frac{P_{sr}}{W} \sum_{k=1}^{K} d_k \sum_{i=1}^{N} c_k(i) c_l(i) rect(i) \right] \quad (8)$$

Here, Psr denotes the optical power received at the receiver. The CSD code cross-correlation is given by [10]

$$\sum_{i=1}^{N} c_k(i)c_l(i) = \begin{cases} W, for\, k = l \\ \left|\frac{W}{2}\right|, for \begin{cases} \mathrm{l = k + (K/2), \text{ if } k > l} \\ \mathrm{l = l - (K/2), \text{ if } l > k} \end{cases} \\ 0, otherwise \end{cases} \quad (9)$$

The CSD code exhibits only $W/2$ bits of overlap with any single user among all users in the system. Accordingly, the power spectral density is given by

$$G(v) = \frac{P_{sr}}{\Delta v} \left[W \sum_{k=l} rect(i)\delta(v - v_i) + \frac{W}{2} \sum_{K=\pm K/2} rect(i)\delta(v - v_i) \right] \quad (10)$$

Considering when all transmitters are sending bit '1', $rect(i) = u\left[\frac{\Delta v}{N}\right]$ and so,

$$G(v) = \frac{3P_{sr}W}{2N} \quad (11)$$

Furthermore, for the polarization-multiplexed encoded signal, $G(v)$ is represented as [16]

$$G_x(v) = \alpha e^{j\phi_x} \frac{3P_{sr}W}{2N} \text{ and } \quad G_y(v) = (1-\alpha) e^{j\phi_y} \frac{3P_{sr}W}{2N}$$

The term α denotes the adaptive power-splitting ratio, ideally equal to 0.5, and ϕ represents the phase difference, defined as $\phi x - \phi y$, which is ideally zero. Both parameters are regulated by the adaptive polarization multiplexing mechanism to maintain balanced power and phase between the polarization-split beams.

$$P_r(t) = \Re \frac{3P_{sr}W}{2N} \left[\sqrt{\alpha} e^{j\phi x} \sum_{n=1}^{K} C_n{}^{(x)} e^{j2\pi f_n t} \hat{x} + \sqrt{1-\alpha} e^{j\phi y} \sum_{n=1}^{K} C_n{}^{(y)} e^{j2\pi f_n t} \hat{y} \right]^2$$

Over one symbol duration or multiple OFDM cycles, the cross-terms between different subcarriers average to zero due to their frequency orthogonality. This orthogonality is defined as [6]

$$f_n = \frac{n-1}{k}$$

$$P_r(t) = \Re \frac{3P_{sr}W}{2N} \begin{pmatrix} \alpha\eta_x + (1-\alpha)\eta_y \\ +2\sqrt{\alpha(1-\alpha)\eta_x\eta_x}\, cos(\Delta\phi) \end{pmatrix}^2 \quad (12)$$

The terms η_x and η_y represent the polarization-dependent quantum efficiencies of the detector. The composite signal from the transmitter then propagates through the hybrid amplifier. It is amplified by a total gain G_{hyb} [9]. The received signal power is expressed as

$$\langle i_p{}^2 \rangle = G_{hyb}\, P_{\quad r}(t) \quad (13)$$

Where $G_{hyb} = G_{EDFA} G_{Raman}$

As the signal travels through the fiber channel, it undergoes various forms of noise. At the receiver, the shot noise is denoted as in Equation 14 [4, 6]. The Polarization Dependent Loss (PDL), known as PIIN noise, is denoted as in Equation 15 [10, 12]. These noise components collectively degrade signal quality and increase the BER, thereby limiting system performance.

$$\sigma_{sh}{}^2 = 2eBI = 2eB_e \Re \frac{3P_{sr}W}{2N} \left[\begin{matrix} \alpha\eta_x + \\ (1-\alpha)\eta_y \end{matrix} \right] \quad (14)$$

$$\sigma_{PDL}{}^2 = B_e \Re^2 \frac{9P_{sr}{}^2 W^2}{4N^2} \left[\begin{matrix} \alpha^2\eta_x{}^2 + (1-\alpha)^2\eta_y{}^2 + \\ 2\alpha(1-\alpha)\eta_x\eta_y\, cos\, \Delta\, \phi \end{matrix} \right] \quad 15)$$

The thermal noise at the receiver end is denoted as [13]

$$\sigma_{th}^2 = \frac{4B_e K_B T_n}{R_L} \quad (16)$$

The Amplifier Spontaneous Emission (ASE) noise can be evaluated as [9]

$$\sigma^2{}_{ASE} = n_{sp} hv (G_{hyb} - 1) B_e \left[\alpha\eta_x + (1-\alpha)\eta_y \right] \quad (17)$$

Third-order intensity modulation noise comes from the nonlinear mixing of signal components. It is mainly caused by nonlinear effects in lasers, modulators, and the fiber channel. It is mathematically expressed as [6]

$$\sigma^2_{IMD3} = \Re^2 \, P_{sr} \frac{9}{32} a^2{}_3 A^6 \qquad (18)$$

Where α_3 is the normalized cubic nonlinearity coefficient, and A is the modulation amplitude. By substituting Equations 14 – 18 into Equation 5, the resulting SNR for the system is given by

$$SNR = \frac{\langle I_p{}^2 \rangle}{\sigma_{total}{}^2} = \frac{\Re^2 \frac{3P_{sr}W}{2N} \left(\begin{matrix} \alpha\eta_x + (1-\alpha)\eta_y + \\ 2\sqrt{\alpha(1-\alpha)\eta_x\eta_x}\cos(\Delta\phi) \end{matrix} \right)^2}{\left(\begin{matrix} \frac{4B_e K_B T_n}{R_L} + \Re^2 \\ P_{\frac{9}{32}{}^2{}_3{}^6{}_{sr}} \end{matrix} \quad \sigma_{PDL}{}^2 + \sigma^2{}_{sh} + \sigma_{ASE}{}^2 \right)} \qquad (19)$$

The BER is formulated as a function of the SNR using Equation 12 by [4]

$$BER = 0.5 \, erf\left(\sqrt{\frac{SNR}{2}}\right) \qquad (20)$$

5. Simulation Model

The transmitter uses broadband optical sources to generate a highly coherent and stable optical field. This field is then routed to a polarization splitter module, as illustrated in Figure 2. This specialized block efficiently decomposes the incident beam into two orthogonally polarized components of equivalent intensity.

The separated X- and Y-polarization channels are modulated with user data, which is QPSK-OFDM modulated. The system employs a 128-point FFT, and a cyclic prefix of one-sixteenth of the symbol duration [17, 19].

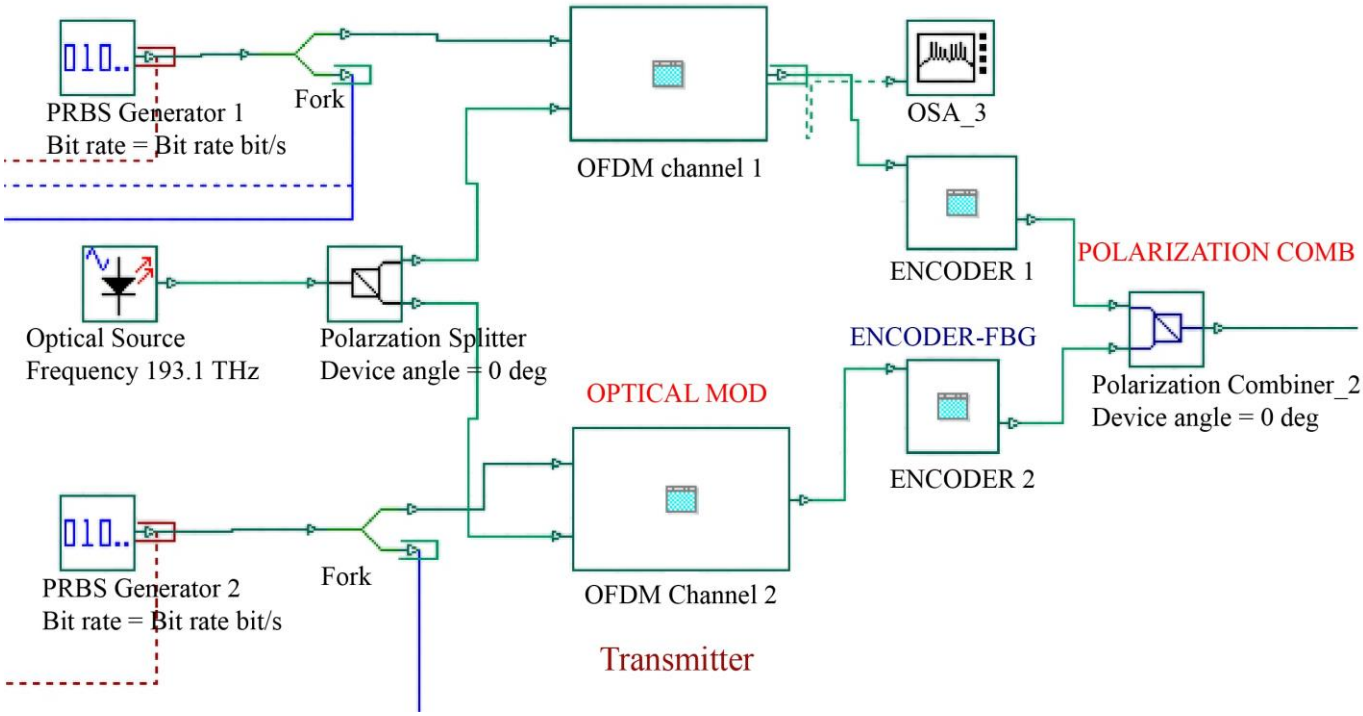

Fig. 2 Transmitter simulation model

Following modulation, each channel is spectrally encoded with robust CSD codes via Fiber Bragg Gratings (FBGs) [3]. The chirp size of each channel must exceed the bandwidth of an OFDM subcarrier, ensuring that the chirped spectral components are properly distinguishable.

The FBGs are tuned to 1550 nm, with a bandwidth of 0.4 nm and 90% reflectivity. Finally, the channels are recombined using a polarization beam combiner to generate the dual-polarization multiplexed optical signal.

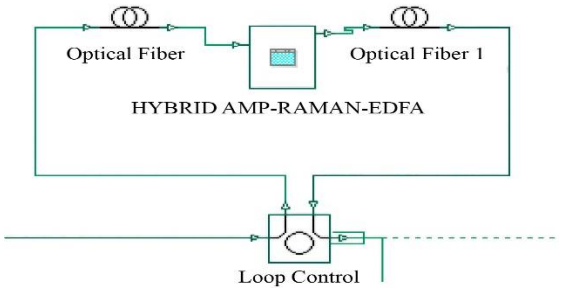

Fig. 3 Channel simulation model

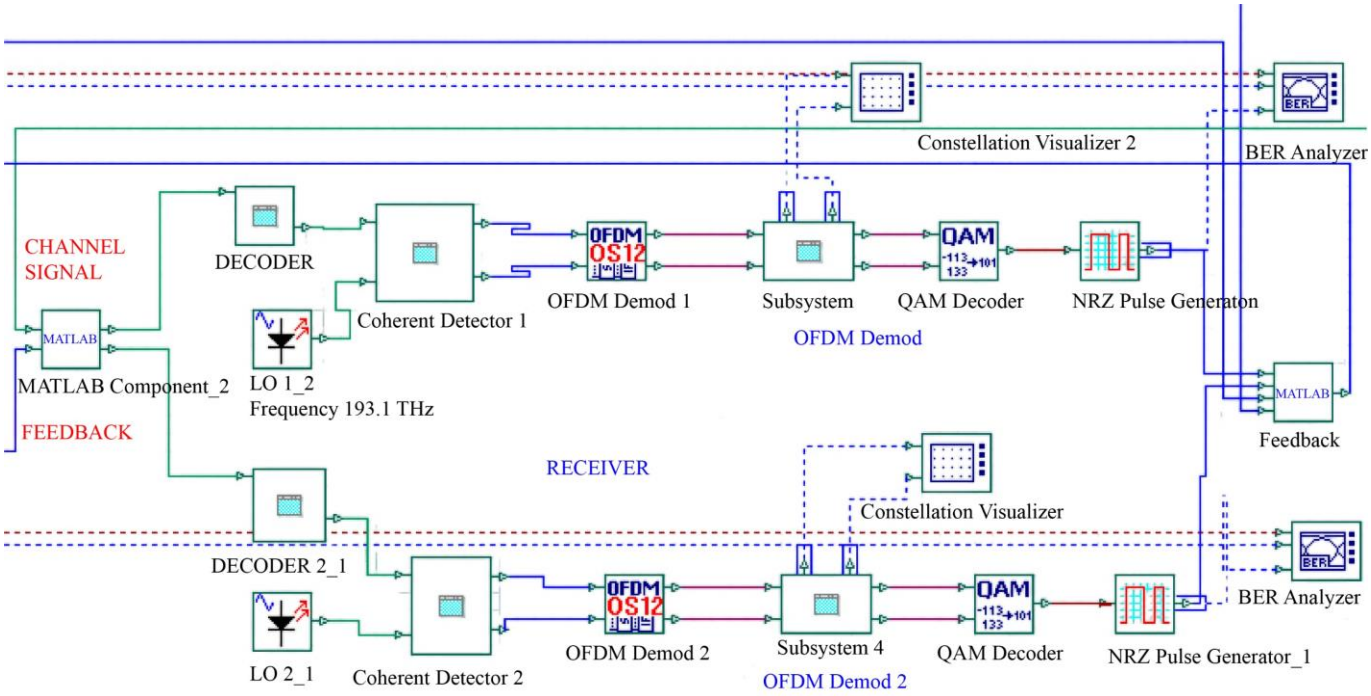

Fig. 4 Receiver simulation model

The aggregated optical signal is sent through a 30 km length of standard single-mode fiber with an attenuation of 0.2 dB/km, a chromatic dispersion of 16 ps/nm/km, and a nonlinearity coefficient of 2.6/W/km as reflected in Figure 3**,** a hybrid amplification scheme is used, with a distributed Raman amplifier over the first 6 km providing 10 dB of gain with 400 mW of pump power at 1450 nm [21]. This is followed by an EDFA with 10 dB gain and a noise figure of 4.5 dB. This Raman-first configuration reduces polarization-dependent loss, improves SNR, and ensures uniform gain before lumped amplification [21]. At the receiver, a MATLAB-based Adaptive polarization demultiplexer separates X and Y components. It adaptively aligns their phase and state using BER feedback. Each polarization stream is decoded using an FBG [3] with the same 1550 nm center wavelength and 0.4 nm bandwidth, ensuring matched filtering. Detection is performed with photodetectors having a responsivity of 0.9 A/W and a bandwidth of 20 GHz.

Figure 4 shows the receiver design of the system. Signals are demodulated using the same QPSK-OFDM parameters as the transmitter, followed by NRZ demodulation [17, 19]. A MATLAB-based BER analyzer averages users' BER. The result is compared with a 10^{-9} threshold. Based on the comparison, it generates feedback to adjust the demultiplexing polarization states for continuous optimization adaptively.

6. Results and Discussion

6.1. Simulation Model Results Discussion

The recovered signal is checked with a BER analyzer. Figure 5(a) shows the eye diagram at the receiver end of user-1. It exhibits a sufficiently open eye, confirming the proposed simulation model's ability to accurately recover the transmitted signal at the receiver over 15 km.

The constellation diagram for the transmitted 4-QAM signal, presented in Figure 5(b), demonstrates clear phase separation for each symbol. It further validates the system's effective signal detection and recovery performance.

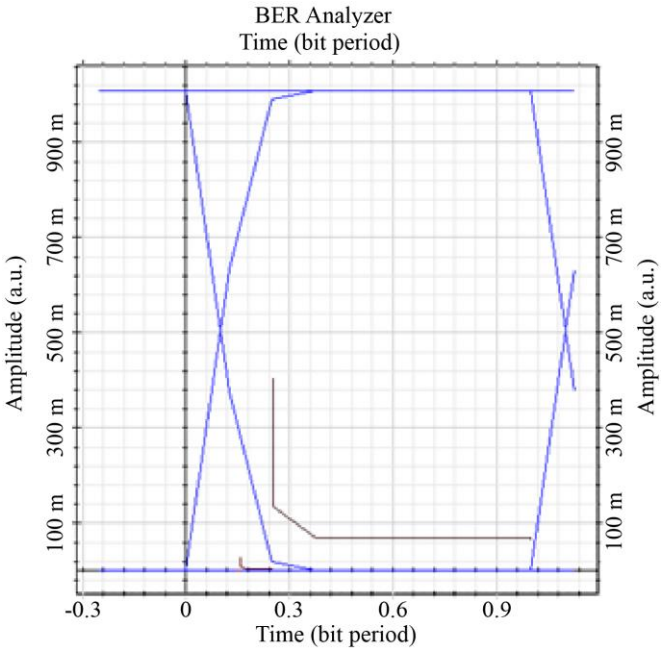

(a)

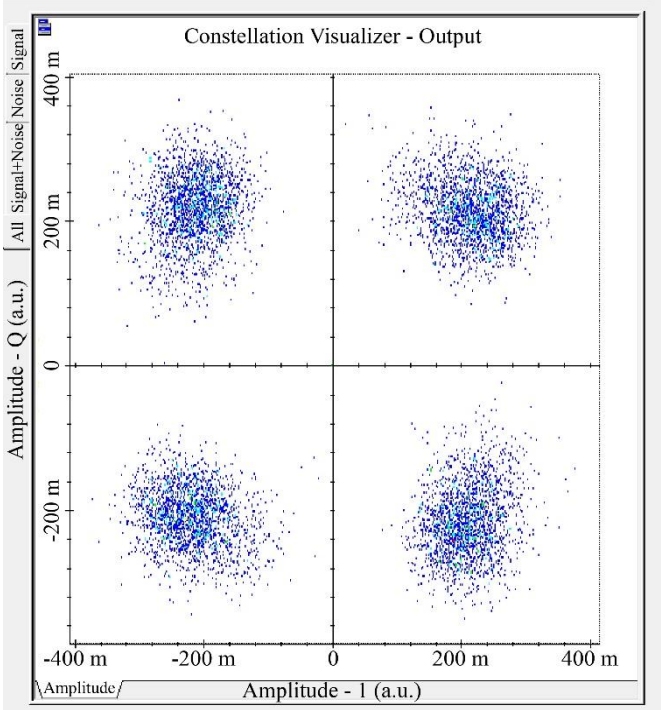

(b)

Fig. 5 Receiver, (a) Eye diagram, and (b) Constellation diagram.

6.2. Analytical Model Results

The performance of the system is assessed by analyzing the BER in relation to both user count and received power levels. The obtained results present a performance comparison of OFDM-OCDMA systems employing ZCC [4, 11] codes, MDW Code [6], and FCC [5] codes with the proposed system. Consequently, the parameters[4-6, 10, 11] in Table 1 are selected based on these three coded systems. The chosen parameters ensure a thorough evaluation of performance across the different systems.

Table 1. Typical system parameters

Parameters	Values
Operating Frequency	193.1 THz
Electrical Bandwidth (B_e)	311 MHz
Linewidth Source (Δv)	3.75 THz
Photodetector Quantum Eff. (η)	0.6
Bit Rate	622 Mbps
Receiver Noise Temp (T_n)	300 K
Receiver Load Resistor (R_L)	1030 Ω
Number of subcarriers	256
Boltzmann's constant (K_b)	6.66×10^{-34} Js
Planck's constant (h)	1.38×10^{-23} J/K
Electron charge (e)	1.6×10^{-19} C
PDL Factors (η_x,η_y)	0.8, 0.7
Amplifiers Gain (G_{hyb})	27 dB

The graph in Figure 6 compares the proposed system with various existing OFDM-OCDMA schemes. Considering a received optical power of -20 dBm and a per-user data rate of 622 Mbps, the proposed adaptive polarization-multiplexed CSD-coded OFDM-OCDMA system supports 184 simultaneous users at the target BER of 10^{-9}, as summarized in Table 1.

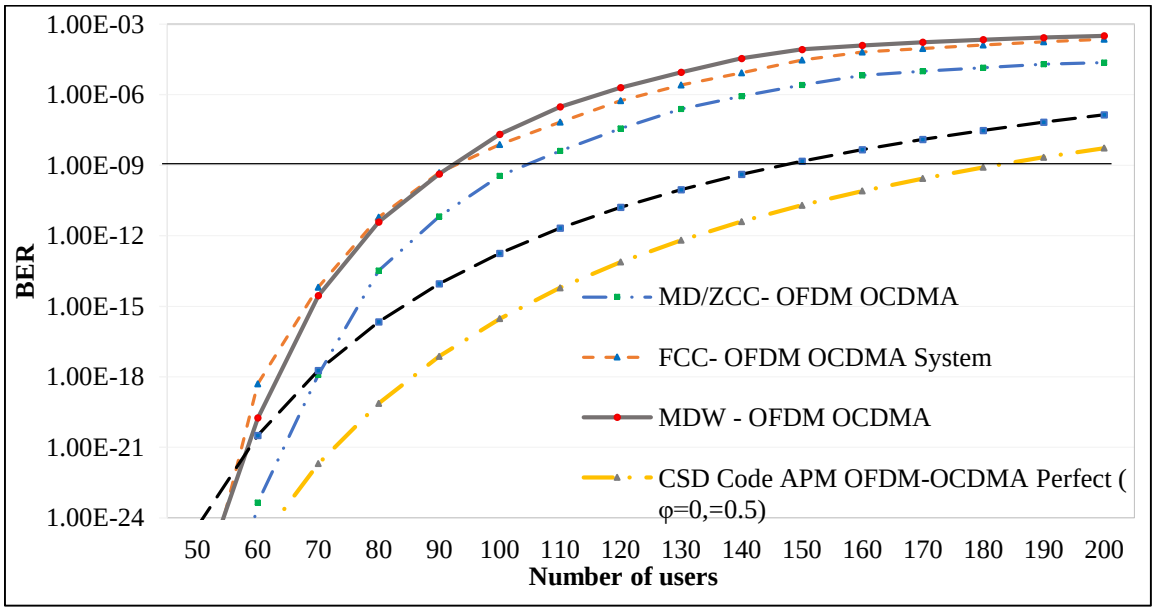

Fig. 6 BER vs. Number of users for different systems

Under the same operating conditions, conventional FCC- and ZCC-coded OFDM-OCDMA systems support only 100 and 107 users, respectively. These limits apply when polarization multiplexing is not employed. Although the longer ZCC code length reduces overall SNR, the shorter FCC code is penalized by elevated cross-correlation. This

compromises receiver spectral density and further degrades SNR performance.

By contrast, the proposed CSD code exhibits negligible cross-correlation and reduced code length. When combined with adaptive polarization multiplexing, the system reaches its optimal polarization settings ($\phi = 0°$ and $\alpha = 0.5$). Under these conditions, it supports up to 184 users, as illustrated in Figure 6. This delivers capacity enhancements of approximately 84% and 72% over FCC- and ZCC-coded systems, respectively.

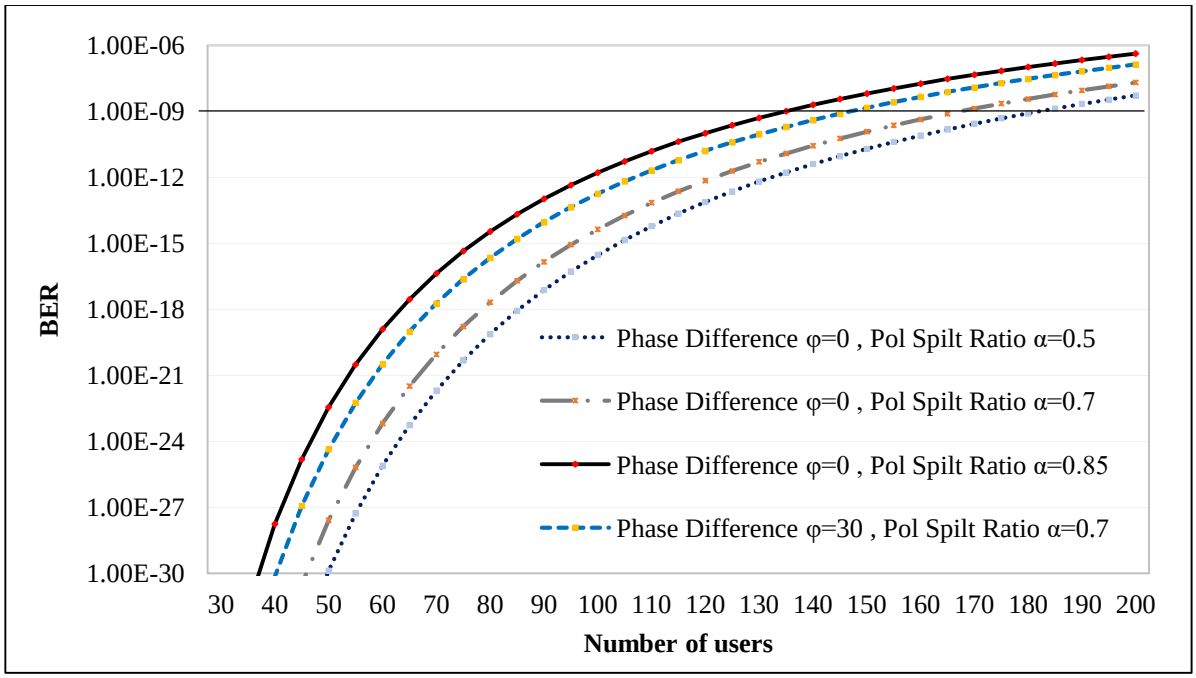

Fig. 7 BER vs. Number of users for variable A

In contrast, deviations such as $\phi = 30°$ and $\alpha = 0.7$ introduce polarization-dependent loss, reducing the supported user count to 146.

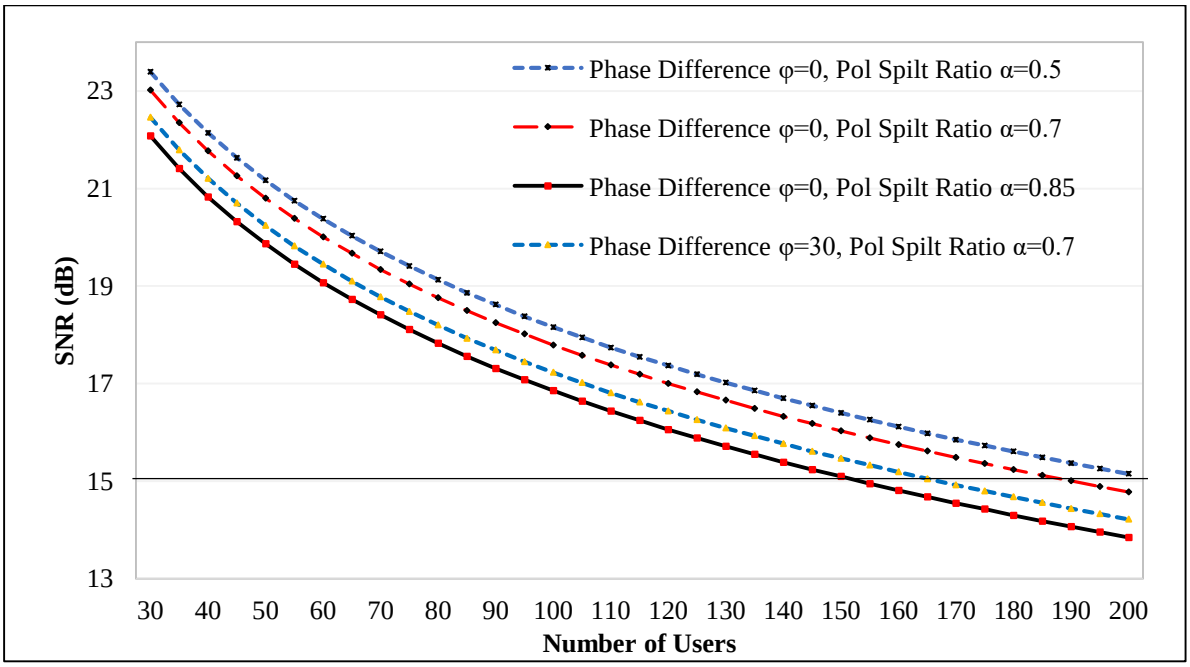

Fig. 8 SNR vs. Number of users for variable α

Figures 7 and 8 depict the influence of polarization split ratio (α) and phase difference (ϕ) on system performance, respectively. The adaptive polarization multiplex block maintains equal channel power, with α = 0.5 supporting 184 users. Increasing α to 0.85 reduces the number of supported users to 134. Minimal ϕ (0°) suppresses polarization leakage distortions, enhancing SNR and reducing BER.

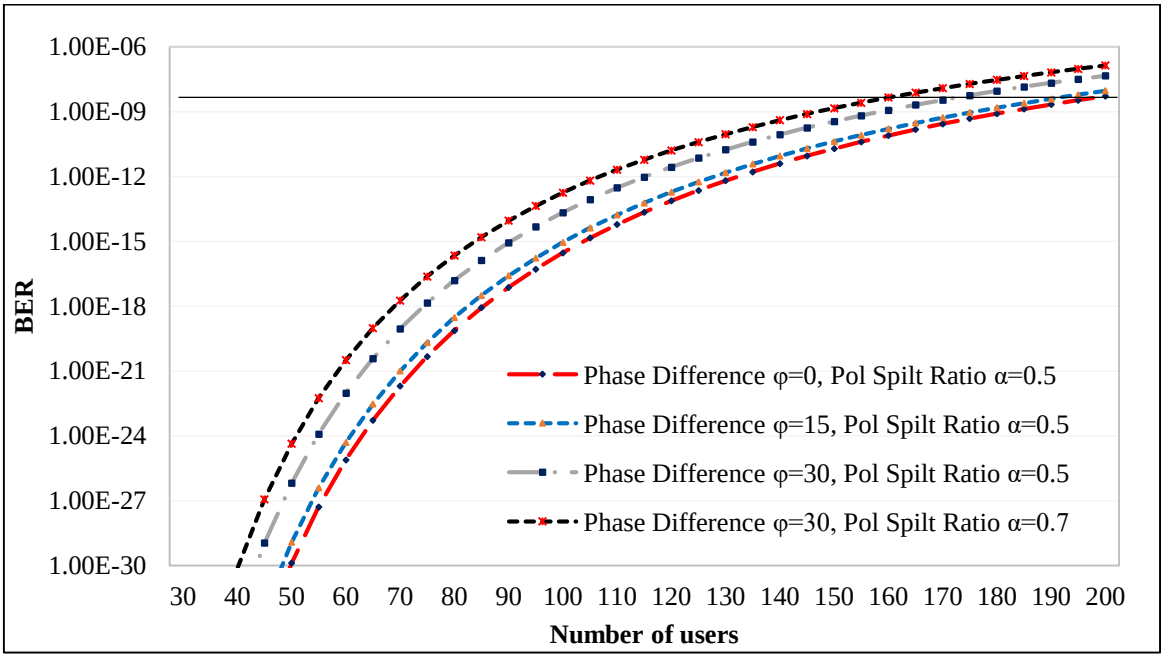

Fig. 9 BER vs. Number of users for variable ϕ

Higher ϕ values cause notable degradation. For ϕ= 0° and the given system parameters, up to 184 users can be accommodated. However, when ϕ varies from 15° to 30°, the maximum number of supported users decreases from 175 to 158, as shown in Figure 9. The proposed adaptive polarization multiplexing block mitigates ϕ variations, thereby maintaining user capacity in the system.

7. Conclusion

The proposed adaptive polarization-multiplexed OFDM-SAC OCDMA system employs a short-length CSD code with negligible cross-correlation. This design shows clear improvements in BER, SNR, and user capacity. The gains are evident when compared with conventional ZCC- and FCC-coded OFDM systems. Under identical conditions at a per-user rate of 622 Mbps and a received power of –20 dBm, the compact CSD code yielded user capacities 72% and 84% higher than those of the ZCC and FCC schemes, respectively. Optimal polarization stability, achieved at α = 0.5 and ϕ = 0°, minimizes polarization-dependent losses. However, deviations such as α = 0.7 and ϕ = 30° reduce the system capacity from 184 to 146 users. Under optimal conditions (α = 0.5, ϕ = 0°), the adaptive polarization multiplexing block maintains equal channel power and supports 184 users. Increasing the polarization split ratio to α = 0.85, however, lowers the supported capacity to 134 users due to polarization-induced SNR loss. Likewise, minimal ϕ (0°) suppresses polarization leakage and enhances SNR, whereas increasing ϕ from 15° to 30° decreases the supported users from 175 to 158. Thus, supported by feedback-controlled gain adjustment, the block dynamically mitigates α and ϕ drifts, ensuring robust performance under load variations. As broadband sources are inherently sensitive to polarization, fiber birefringence limits stable transmission to only a few tens of kilometres. The proposed approach enhances the performance of optical communication systems by enhancing spectral efficiency and mitigating polarization-dependent impairments. It further maintains robust SNR under dynamic network conditions in metropolitan area networks.

References

[1] Samia Driz, and Benattou Fassi, "Enhancing QS – SAC – OCDMA Networks Capacity via 2D Spectral/Polarization OZCZ Coding Technique Based on Modified Pascal's Triangle Matrix," *Optical and Quantum Electronics*, vol. 54, 2022. [CrossRef] [Google Scholar] [Publisher Link]

[2] Mohamed Rahmani et al., "Performance Investigation of 1.5 Tb/s Optical Hybrid 2D-OCDMA/OFDM System Using Direct Spectral Detection based on Successive Weight Encoding Algorithm," *Optics & Laser Technology*, vol. 174, 2024. [CrossRef] [Google Scholar] [Publisher Link]

[3] Hichem Mrabet, "A Performance Analysis of a Hybrid OCDMA-PON Configuration Based on IM/DD Fast-OFDM Technique for Access Network," *Applied Sciences*, vol. 10, no. 21, pp. 1-13, 2020. [CrossRef] [Google Scholar] [Publisher Link]

[4] Mohamed Rahmani et al., "Contribution of OFDM Modulation to Improve the Performance of Non-Coherent OCDMA System based on a New Variable Weight Zero Cross Correlation Code," *Optical and Quantum Electronics*, vol. 54, 2022. [CrossRef] [Google Scholar] [Publisher Link]

[5] A.O. Aldhaibani et al., "Development of OCDMA System based on Flexible Cross Correlation (FCC) Code with OFDM Modulation," *Optical Fiber Technology*, vol. 22, pp. 7-12, 2015. [CrossRef] [Google Scholar] [Publisher Link]

[6] A.O. Aldhaibani et al., "A New Model to Enhance the QoS of Spectral Amplitude Coding-Optical Code Division Multiple Access System with OFDM Technique," *Optical and Quantum Electronics*, vol. 48, pp. 1-12, 2016. [CrossRef] [Google Scholar] [Publisher Link]

[7] Ammar Armghan et al., "Performance Analysis of Hybrid PDM-SAC-OCDMA Enabled FSO Transmission Using ZCC Codes," *Applied Sciences*, vol. 13, no. 5, pp. 1-14, 2023. [CrossRef] [Google Scholar] [Publisher Link]

[8] Zhi-Yu Chen et al., "Use of Polarization Freedom Beyond Polarization-Division Multiplexing to Support High-Speed and Spectral-Efficient Data Transmission," *Light: Science & Applications*, vol. 6, pp. 1-7, 2017. [CrossRef] [Google Scholar] [Publisher Link]

[9] Amit Wason, and Deepak Malik, "Performance Investigation of Hybrid Optical Amplifiers for High-Speed Optical Networks," *Journal of Optics*, vol. 49, pp. 298-304, 2020. [CrossRef] [Google Scholar] [Publisher Link]

[10] Nabiha Jellali, Moez Ferchichi, and Monia Najjar, "4D Encoding Scheme for OCDMA System Based On Multi-Diagonal Code," *Optik*, vol. 244, 2021. [CrossRef] [Google Scholar] [Publisher Link]

[11] Bedir Yousif, Ibrahim El. Metwally, and Ahmed Shaban Samra, "A Modified Topology Achieved in OFDM/SAC-OCDMA-based Multi-Diagonal Code for Enhancing Spectral Efficiency," *Photonic Network Communications*, vol. 37, pp. 90-99, 2019. [CrossRef] [Google Scholar] [Publisher Link]

[12] S. Boukricha et al., "SAC-OCDMA System Performance Using Narrowband Bragg Filter Encoders and Decoders," *SN Applied Sciences*, vol. 2, pp. 1-9, 2020. [CrossRef] [Google Scholar] [Publisher Link]

[13] Zou Wei, and H. Ghafouri-Shiraz, "Codes for Spectral-Amplitude Coding Optical CDMA Systems," *Journal of Lightwave Technology*, vol. 20, no. 8, pp. 1284-1291, 2002. [CrossRef] [Google Scholar] [Publisher Link]

[14] A. Garadi, A. Djebbari, and Taleb-Ahmed Abdelmalik, "Exact Analysis of Signal-to-Noise Ratio for SAC-OCDMA System with Direct Detection," *Optik*, vol. 145, pp. 89-94, 2017. [CrossRef] [Google Scholar] [Publisher Link]

[15] Syed Mohammad Ammar et al., "Development of New Spectral Amplitude Coding OCDMA Code by Using Polarization Encoding Technique," *Applied Sciences*, vol. 13, no. 5, pp. 1-15, 2023. [CrossRef] [Google Scholar] [Publisher Link]

[16] Ahmed Garadi et al., "Enhanced Performances of SAC-OCDMA System by Using Polarization Encoding," *Journal of Optical Communications*, vol. 41, no. 3, pp. 319-324, 2020. [CrossRef] [Google Scholar] [Publisher Link]

[17] Chih-Ta Yen, and Wen-Bin Chen, "A Study of Dispersion Compensation of Polarization Multiplexing-based OFDM-OCDMA for Radio-Over-Fiber Transmissions," *Sensors*, vol. 16, no. 9, pp. pp. 1-16, 2016. [CrossRef] [Google Scholar] [Publisher Link]

[18] Chongfu Zhang et al., "Polarization Multiplexed OFDM Band Interleaving Enabled Metro-Access Integrated Networks," *Optical Fiber Technology*, vol. 20, no. 2, pp. 130-136, 2014. [CrossRef] [Google Scholar] [Publisher Link]

[19] X. Guo et al., "High Speed OFDM-CDMA Optical Access Network," *Optics Letters*, vol. 41, no. 8, pp. 1809-1812, 2016. [CrossRef] [Google Scholar] [Publisher Link]

[20] Kuanlin Mu et al., "Raman/EDFA Hybrid Bidirectional Amplifier for Fiber-Optic Time and Frequency Synchronization," *Optics Express*, vol. 29, no. 5, pp. 6356-6367, 2021. [CrossRef] [Google Scholar] [Publisher Link]

[21] Simranjit Singh, and Rajinder Singh Kaler, "Review on Recent Developments in Hybrid Optical Amplifier for Dense Wavelength Division Multiplexed System," *Optical Engineering*, vol. 54, no. 10, pp. 1-12, 2015. [CrossRef] [Google Scholar] [Publisher Link]